Original Article

Low dose cone-beam computed tomography reconstruction via hybrid prior contour based total variation regularization (hybrid-PCTV)

Yingxuan Chen[1], Fang-Fang Yin[1,2,3], Yawei Zhang[2], You Zhang[1], Lei Ren[1,2]

[1]Medical Physics Graduate Program, Duke University, Durham, NC, USA; [2]Department of Radiation Oncology, Duke University Medical Center, Durham, NC, USA; [3]Medical Physics Graduate Program, Duke Kunshan University, Kunshan 215316, China

Correspondence to: Lei Ren. Department of Radiation Oncology, Duke University Medical Center, DUMC Box 3295, Durham, North Carolina 27710, USA. Email: lei.ren@duke.edu.

Background: Previously, we developed a prior contour based total variation (PCTV) method to use edge information derived from prior images for edge enhancement in low-dose cone-beam computed tomography (CBCT) reconstruction. However, the accuracy of edge enhancement in PCTV is affected by the deformable registration errors and anatomical changes from prior to on-board images. In this study, we develop a hybrid-PCTV method to address this limitation to enhance the robustness and accuracy of the PCTV method.

Methods: Planning-CT is used as prior images and deformably registered with on-board CBCT reconstructed by the edge preserving TV (EPTV) method. Edges derived from planning CT are deformed based on the registered deformation vector fields to generate on-board edges for edge enhancement in PCTV reconstruction. Reference CBCT is reconstructed from the simulated projections of the deformed planning-CT. Image similarity map is then calculated between reference and on-board CBCT using structural similarity index (SSIM) method to estimate local registration accuracy. The hybrid-PCTV method enhances the edge information based on a weighted edge map that combines edges from both PCTV and EPTV methods. Higher weighting is given to PCTV edges at regions with high registration accuracy and to EPTV edges at regions with low registration accuracy. The hybrid-PCTV method was evaluated using both digital extended-cardiac-torso (XCAT) phantom and lung patient data. In XCAT study, breathing amplitude change, tumor shrinkage and new tumor were simulated from CT to CBCT. In the patient study, both simulated and real projections of lung patients were used for reconstruction. Results were compared with both EPTV and PCTV methods.

Results: EPTV led to blurring bony structures due to missing edge information, and PCTV led to blurring tumor edges due to inaccurate edge information caused by errors in the deformable registration. In contrast, hybrid-PCTV enhanced edges of both bone and tumor. In XCAT study using 30 half-fan CBCT projections, compared with ground truth, relative errors (REs) were 1.3%, 1.1% and 0.9% and edge cross-correlation were 0.66, 0.68 and 0.71 for EPTV, PCTV and hybrid-PCTV, respectively. Moreover, in the lung patient data, hybrid-PCTV avoided the wrong edge enhancement in the PCTV method while maintaining enhancements of the correct edges.

Conclusions: Hybrid-PCTV further improved the robustness and accuracy of PCTV by accounting for uncertainties in deformable registration and anatomical changes between prior and onboard images. The accurate edge enhancement in hybrid-PCTV will be valuable for target localization in radiation therapy.

Keywords: Cone-beam computed tomography (CBCT); low dose reconstruction; total variation

Submitted Apr 04, 2019. Accepted for publication May 26, 2019.
doi: 10.21037/qims.2019.06.02
View this article at: http://dx.doi.org/10.21037/qims.2019.06.02

Introduction

Target localization accuracy is critical for radiation therapy, since it is correlated with tumor control and normal tissue toxicity. It is especially important for the lung and liver cancer treatments, which are prone to localization errors caused by respiratory motions (1-4). Cone-beam computed tomography (CBCT) is the most widely used imaging technique to provide image guidance for target localization to improve the treatment delivery accuracy. 3D breath-hold CBCT is used for the patients treated with breath-hold, while 4D CBCT is used for patients treated with free breathing. In clinical practice, it is often needed to acquire CBCT with under sampled projections to reduce its imaging dose and scanning time. For example, a clinical 3D CBCT scan takes 1 minute and delivers imaging dose around 2–3 cGy through a large volume of the body (5). Repeating 3D CBCT scans multiple times for inter- and intra-fraction verification would lead to long scanning time and high imaging dose, which are not optimal for patient care. Reducing the number of projections when acquiring a 3D CBCT can potentially reduce the imaging dose and also improve imaging efficiency. In clinical 4D CBCT scans, the projections acquired for each respiratory phase are always undersampled to only 100–200 projections with the total scanning time of 4 minutes and imaging dose of ~6 cGy (dose rates of 3.0×10^{-3} cGy/mAs at isocenter) (6). Further reducing the projection number can reduce the scanning time and dose even more to make it feasible to acquire multiple 4D-CBCT scans for intra-fraction verification.

Reconstructing CBCT from under-sampled projections is challenging. For example, CBCT reconstructed by the conventional Feldkamp, Davis, and Kress (FDK) algorithm (7) suffers from severe streak artifacts due to the under-sampling. Compressed sensing methods have been developed in the past decade for the low dose CT/CBCT reconstruction. Among these methods, total variation (TV) or total generalized variation (TGV) were widely used as regularization to reduce streak artifacts and noise (8-12). However, edge information tends to be over-smoothed by uniformly penalizing the image gradient using TV/TGV regularization (13), which limits the performance of these methods in the low-dose reconstruction. To overcome this limitation, weighted TV methods were developed for both MR and CT reconstruction to enhance edges in the final images (14-18). The low weight of TV penalty was designed for the edge region to reduce TV minimization. For example, edge preserving TV (EPTV) (14) was proposed to reduce the blurriness at edge regions by deriving the isotropic edges expressed as the exponential function of image gradient of the intermediate images generated during the iterative reconstruction. Besides EPTV, TV weight map from intermediate images can be calculated in various ways such as deriving anisotropic edges (16); normalizing the TV weighting term by the image gradient (17,18) and reweighted anisotropic TV (19). The main limitation of these methods is that the capability of deriving edge information is limited by the quality of the intermediate images. Thus, edges can be still blurred and small structures can still be missing when using these adaptively weighted TV methods to reconstruct CBCT from a relatively low number of projections (14). Prior image based anisotropic edge guided TV (PIEGTV) (20) was then proposed by simply using prior edge information as initial weights to improve the performance of anisotropic edge guided TV (16).

Another major category of methods is to use prior images to improve the image quality for low dose CT/CBCT reconstruction (21-24). In the prior image constrained compressed sensing (PICCS) (22) method, sampling requirement was reduced with prior images used as an additional constraint to minimize image TV. Moreover, we developed a limited-angle intra-fraction verification (LIVE) system to use prior images and deformation models to estimate on-board CBCT from limited angle projections (25-29). Furthermore, methods were developed to account for the mismatch between prior image and on-board CBCT by using adaptively weighted constraint (23,24,30) or registration (rigid or deformable) between the prior and on-board image in the reconstruction framework for compensation (31-33). In principle, the quality of the CBCT can be improved using information from the prior images. The management of prior information and current measurement is important to the reconstruction accuracy of such methods.

Previously, we proposed a prior contour based TV (PCTV) method, which uses the edge information from high-quality prior images and image registration to generate on-board edges for edge enhancement in on-board CBCT reconstruction (13). While edges were enhanced compared to previous TV and EPTV methods, a limitation of the PCTV method is that edge enhancement in the reconstructed images may be affected by the accuracy of registration, especially when deformation exists. Moreover, if an anatomical change such as tumor shrinkage occurs, deformed prior contour information may not be accurate to reflect the on-board edges, which will affect the accuracy of

the edge enhancement in the reconstruction.

In this study, a hybrid-PCTV method was developed to account for the registration errors in the PCTV reconstruction. Specifically, the hybrid-PCTV method combines PCTV edges with EPTV edges based on the local estimation of the registration errors and anatomical mismatches between prior image and on-board volume. The new hybrid-PCTV method was compared with EPTV and PCTV using digital 4D lung phantom, clinical simulated digitally reconstructed radiography (DRR) and real projections of lung patient data with both qualitative and quantitative evaluations. The results indicated that the new hybrid-PCTV method improved the accuracy and robustness of the PCTV method against deformable registration errors and anatomical changes between prior and on-board volumes.

Methods

Prior contour based TV reconstruction

TV is defined as the integration of the image gradient magnitude and has been widely used as a regularization term in the compressed sensing reconstruction. The goal of TV based reconstruction is to minimize the TV of the image being reconstructed:

$$f^* = \arg\min \|f\|_{TV} \quad [1]$$

Subject to the data fidelity constraint:

$$\|DRR(f) - Proj\|_2^2 \leq \epsilon \quad [2]$$

where f is the image to be reconstructed, and DRR(f) is forward projection of image f. *Proj* represents the on-board CBCT projections acquired. Streak artifacts and noise in the under-sampled CT/CBCT reconstruction can be effectively reduced by the TV regularization. However, edges might be over-smoothed by the uniform gradient penalties. Previously, our propos PCTV method was developed to solve this problem by weighting TV term based on the edge information from the prior images. Sufficient edge information was exacted from high-quality prior CT image to guide the edge enhancement in on-board images. To match the prior edge information to the on-board volume, on-board edge map is then generated from the prior edge map after the rigid or deformable registration between prior and on-board. Low weight will be given in the edge region to reduce TV minimization to enhance the edge sharpness. Our proposed PCTV can better enhance the edge sharpness and recover small structure than other TV weighted methods because of more edge information exacted from prior images. However, the accuracy of the on-board edge weight map is affected by registration accuracy, which might limit the application of the PCTV reconstruction method (13).

Hybrid Prior contour based TV reconstruction

The hybrid-PCTV aims to optimize the on-board edge weight map using hybrid edge weight map to minimize the effect of registration errors. The on-board edge information was modified based on the registration accuracy and was used for weighting TV term in the reconstruction accurately.

As shown in *Figure 1*, hybrid-PCTV is implemented in the following steps:

(I) PCTV weight map generation: planning-CT is registered with on-board CBCT reconstructed with EPTV method through deformable registration. Edge information is detected form prior CT and deformed based on the registration to obtain on-board contours. PCTV weight map is converted from the on-board contours to give low weight for TV minimization near the edges. Details about the PCTV weight map generation were described in the previous publication (13).

(II) EPTV weight map generation: during the reconstruction, the edge information can be detected based on the image gradient of the intermediate results and EPTV weight map is calculated using the same formula described by Tian *et al.* (14).

(III) Balance map α generation: The balance map α is generated to balance between the PCTV and EPTV weight maps when combining them in the hybrid method. Specifically, the balance map α gives high weighting to PCTV at regions with high registration accuracy and high weighting to EPTV at regions with low registration accuracy. The registration accuracy is quantified by calculating the similarity between on-board CBCT and deformed prior CT image. However, the quality of the CT and under-sampled CBCT can be quite different due to the under-sampling and cone-beam geometry, the similarity measure between them is affected by this image quality difference and may not fully represent the registration accuracy. Therefore, in our study, reference CBCT was generated in the same way that on-board CBCT is

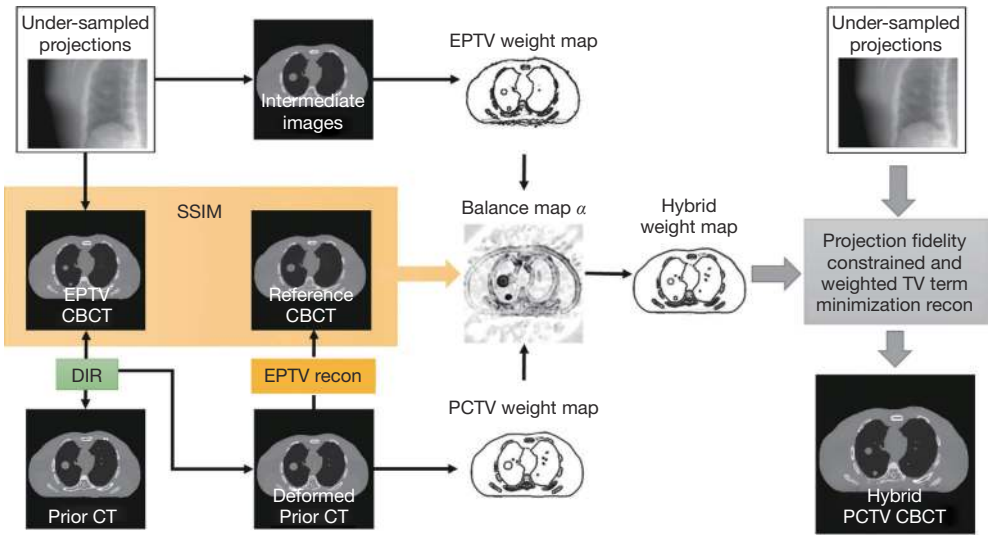

Figure 1 The general workflow of the hybrid-PCTV method. PCTV, prior contour based total variation. EPTV, edge preserving TV; CBCT, cone-beam computed tomography; DIR, deformable image registration.

generated to minimize the image quality difference between reference and on-board images. In this way, the similarity measure can reflect registration accuracy more accurately. The structural similarity index (SSIM) map (34) was used as the metric for the local similarity calculation. A local window is defined at each pixel, and balance map α for each pixel over the entire image is equal to SSIM index calculated within each local window. The isotropic Gaussian filter is used for weighting the neighborhood pixels around a pixel to avoid blocking artifacts in the local estimation. Local window size is determined by the radius, which is the standard deviation of the Gaussian function. In this study, SSIM function built in MATLAB (The MathWorks, Inc., Natick, MA) is used with default settings. Exponents for the luminance, contrast, and structural terms are set to 1 to adjust the importance of these three components to the same level.

(IV) Hybrid weight map generation: hybrid weight map is generated by combining the PCTV weight map and EPTV weight map based on the balance map α. Eq. [3] shows the formula for generating the hybrid weight map.

$$w_{Hybrid}(x) = [1-\alpha(x)] \cdot w_{EPTV}(x) + \alpha(x) \cdot w_{PCTV}(x) \quad [3]$$

PCTV edges will be applied in the regions with high similarity indicating high registration accuracy, while EPTV edges will be applied in the regions with low similarity indicating low registration accuracy.

(V) Hybrid-PCTV reconstruction: The hybrid weight map, $w_{Hybrid}(x)$ in Eq. [3], is used as a TV regularization term to reduce the TV minimization enforcement at the edges in hybrid-PCTV reconstruction.

$$\text{hybrid}-\text{PCTV}(f) = \int w_{Hybrid}(x) \left\| \nabla f(x) \right\|_2 dx \quad [4]$$

The ASD-POCS (9) algorithm was used in the hybrid-PCTV iterative reconstruction to balance the minimization of hybrid-PCTV defined in Eq. [4] and the data fidelity constraints in Eq. [2].

Evaluation studies

Extended cardiac-torso (XCAT) simulation study

4D XCAT is a digital anthropomorphic phantom built based on anatomical datasets from the National Library of Medicine (35). Respiratory motions and sphere lesions can be simulated using this digital phantom to evaluate our method. To simulate 4D images, totally ten phase's images were generated by using specific anatomical parameters and respiratory profiles. The motion in the superior-inferior (SI) direction and in the anterior-posterior (AP) direction were determined by the respiratory profiles including two main curves (diaphragm curve and chest wall curve). The

body and the inserted lesions used the same breathing curve in this project. Both prior 4D-CT set and onboard ground truth 4D-CBCT were simulated with different breathing amplitudes. In addition, lesion diameter was reduced from CT to CBCT and new lesion was inserted in the CBCT to simulate anatomical changes.

Prior 4D-CT simulation

Ten-phase 4D CT was first simulated by using XCAT with a 30 mm diameter spherical lesion inserted in the right lung region. The breathing peak-to-peak respiratory motion amplitudes were set to 3 cm in SI direction and 2 cm in AP direction, respectively.

On-board volume and CBCT projection simulation

The diameter of the lesion in the prior CT was shrinking to 20 mm and a new lesion with 10mm diameter was inserted posteriorly to the first lesion in the right lung region. The breathing peak-to-peak amplitude of on-board volume was changed to 2 cm in the SI direction and 1.2 cm in the AP direction. Half-fan on-board projections were simulated using the Siddon's ray-tracing technique based on on-board volume covering 360° for CBCT reconstruction in cone-beam geometry, which is based on the TrueBeam machine (Varian Medical Systems, Inc., Palo Alto, CA). The distance between source and detector was set to 150 cm and the distance between the source and isocenter was 100 cm. The detector was shifted 16 cm for half-fan mode acquisition. The matrix size for each projection was 512×384 pixels and each pixel size was 0.78×0.78 mm^2.

Deformable registration was performed between the corresponding phases of the prior 4D CT and TV reconstructed 4D-CBCT using Velocity (Varian Medical Systems, Inc., Palo Alto, CA). Single resolution deformable registration was applied due to simplicity of the geometry. In addition, region of interest (ROI) was manually selected for the deformable registration optimization to achieve optimal registration. ROI selection starts with large size to cover whole body as well as eliminate the irrelevant background. And then, small ROI was used to focus on specific region mapping such as target region mapping. Usually, two or three deformable registration optimizations were performed and results were checked manually. After registration, the deformation vector field was generated to transform the prior contour map to the on-board contour map to generate the PCTV weight map. Finally, the hybrid weight map was calculated from EPTV and PCTV weight maps for the hybrid-PCTV reconstruction. The image size for both CBCT and CT volumes at each phase was 256×256×150 voxels and the voxel size was 1.67×1.67×1.67 mm^3.

Effects of projection number

To investigate the effect of projection number on the reconstruction accuracy, 24 (15° per projection), 30 (12° per projection) and 36 (10° per projection) half-fan projections were simulated and reconstructed with EPTV, PCTV and hybrid-PCTV for evaluation and comparison.

Patient study using simulated CBCT projections

In this study, two breath-hold CT scans were acquired before and in the middle of the treatment course for lung cancer patients under an IRB-approved protocol. The first CT set was used as the prior CT images, and the second CT set was used to simulate on-board images. Forty-five half-fan CBCT projections over 360° were simulated from the second CT for CBCT reconstruction. Prior contour was extracted from the prior image using edge detection. Prior CT was registered to the EPTV reconstructed CBCT images using deformable registration via Velocity. Unlike the XCAT study, deformable multi pass was used to deform image with more complex structures. Two or three deformation optimizations were applied with ROIs selected manually to map prior CT and on-board EPTV reconstructed CBCT. Reference CBCT was then reconstructed using DRR of the prior CT using EPTV with the same parameters. Similarity balance map α was calculated based on the local similarity between reference CBCT and EPTV and used to form hybrid-PCTV weight map in our proposed method. In this case, the contrast material in the stomach region is different between prior image and on-board image as shown in *Figure 2*. The simulated CBCT projections were reconstructed by EPTV, PCTV and hybrid-PCTV methods to evaluated reconstruction accuracy when the mismatch of the prior image and on-board geometry exists. The image size for both CBCT and CT volumes was 256×256×40 voxels and the voxel size was 1.5234×1.5234×2 mm^3.

Patient study using real CBCT projections

In this study, clinically acquired images of a lung patient treated with stereotactic body radiation therapy were used. Specifically, the images included planning CT acquired on Philips CT simulator (Philips Medical Equipment, Inc., Andover, MA) and real CBCT projections acquired with breath-hold on a Varian TrueBeam machine. Planning CT was acquired and reconstructed with 512×512×148 volume and the voxel size of 1.1719×1.1719×3 mm^3 and used as prior CT. On-board half-fan projections with a clinical protocol (20 mA/15 ms per projection, 125 kVp) were

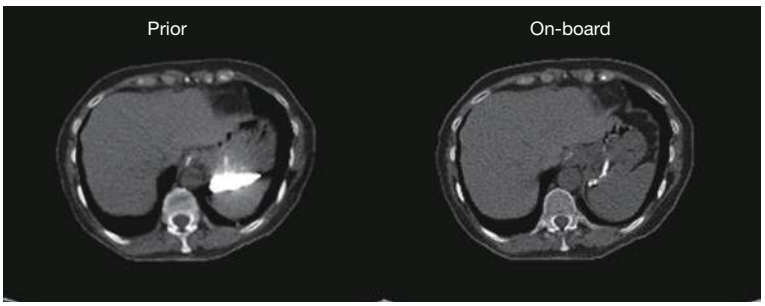

Figure 2 Left is the 1st set CT used as prior image and right is the 2nd set CT used to generate digitally reconstructed radiography (DRR) for reconstruction.

acquired over 360° angle. A total of 894 CBCT half-fan projections were used to reconstruct the reference images via off-line FDK reconstruction algorithm. Prior contour was generated via edge detection. Prior CT was registered to TV based CBCT via Velocity, and deformation vector field was used for PCTV weight map generation. Hybrid weight map was combined PCTV weight map and on-board EPTV weight map based on the similarity between reference CBCT and on-board CBCT reconstructed via EPTV. To investigate the improvement of the hybrid-PCTV method for various under-sampled projections, 111, 149 and 223 half-fan projections (the projection number reduction factors is 8, 6 and 4 respectively) were extracted and used to reconstruct CBCT based on EPTV, PCTV and hybrid-PCTV methods for evaluation. Reconstructed CBCT volume was 400×400×80 with the same voxel size of 1.1719×1.1719×3 mm^3 with the planning breath-hold CT.

Evaluation methods

In the digital XCAT study, both qualitative and quantitative evaluation were used to compare the reconstruction results from EPTV, PCTV and hybrid-PCTV methods. Edge sharpness of two inserted tumors, bone edge sharpness and small structure recovery in the simulated on-board CBCT were evaluated visually as well as via image profile comparison. In addition, the quantitative evaluation was applied in the XCAT study by calculating the relative error (RE) and edge cross correlation coefficient (ECCC) between the reconstructed images and ground truth images as described in (14). A whole image ROI of 90 central slices was defined to contain the entire lung region of XCAT phantom to calculate RE and ECCC. RE is the RE calculated within the defined ROI volume, while ECCC is the mean value of edge cross correlation index of each slice in the ROI volume. In addition, three small ROIs were defined around the spine and two tumors to evaluate local image quality using RE. For other clinical data study, due to the lack of the ground truth, the results in the other studies were compared qualitatively. In the patient study using simulated projections, overall image quality was compared, especially in the mismatched region in the stomach region to evaluate the effect of wrong edge information. In the patient study using real CBCT projections, tumor edge sharpness, structures in the lung and bone edge sharpness were compared with different reconstruction algorithms.

Results

XCAT simulation

Edge enhancement with hybrid-PCTV

CBCT images were reconstructed from 30 noise-free XCAT projections with EPTV, previously proposed PCTV and our hybrid-PCTV methods, and were compared with the ground truth as shown in *Figure 3*.

All methods were capable of enhancing edge sharpness with limited projections. However, the EPTV method was not able to reconstruct some small structures in the lung and over-smoothed bone edges. Moreover, EPTV enhanced streak artifacts as it treats high image gradient as edge in the under-sampled reconstruction. Compared with EPTV, PCTV can recover small structures and enhance the bone. However, as the tumor shrinkage and new tumor growth existed from prior CT to the on-board, PCTV failed to enhance the sharpness of the two tumors because of the inaccurate edge information from the deformed prior CT image. Compared to EPTV and PCTV, the hybrid-PCTV method is capable of recovering small structures as well as enhancing bone and tumor edge information as shown in *Figure 3A* and *B*.

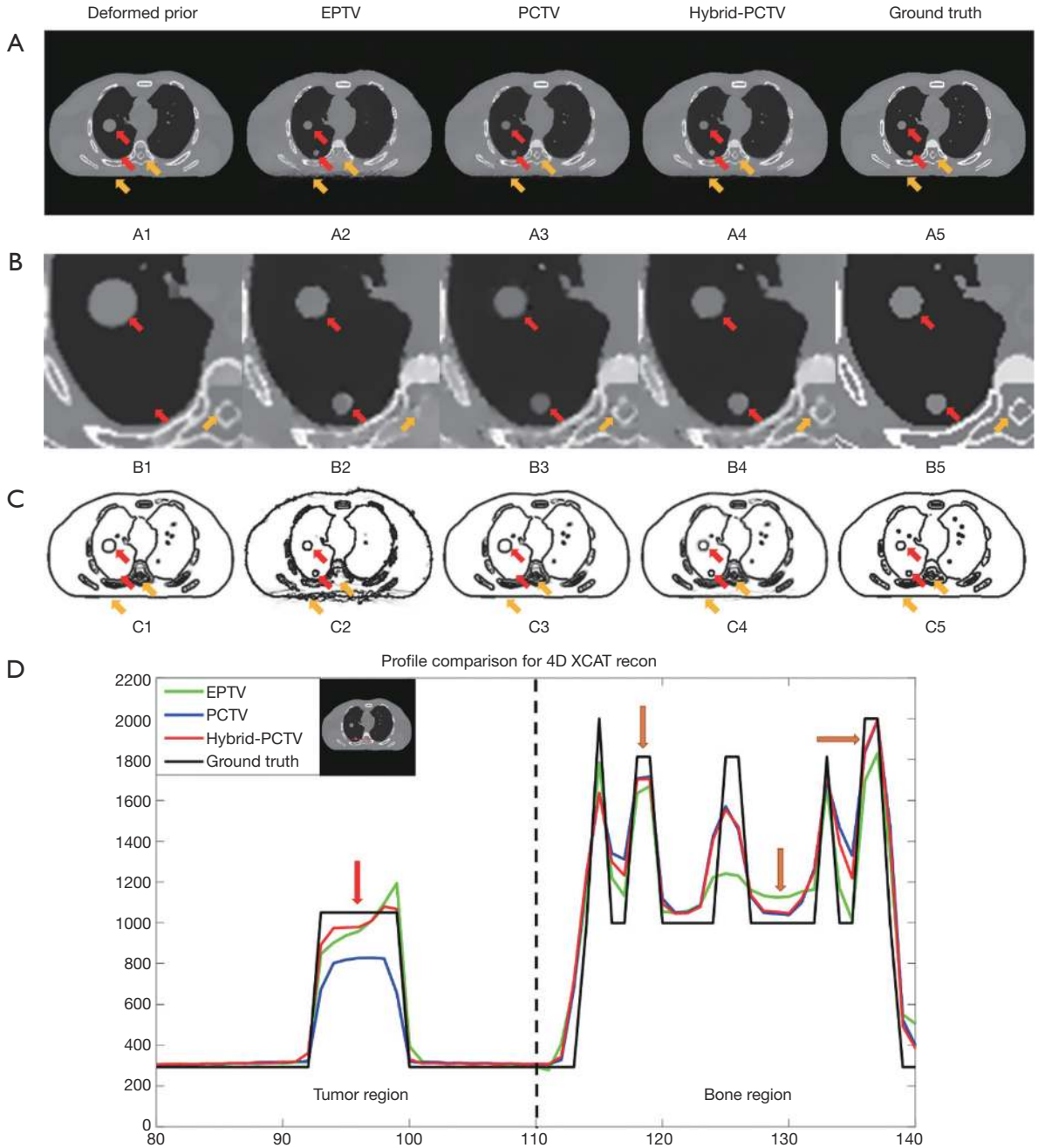

Figure 3 Reconstructed XCAT images using 30 noise free projections and the deformed prior images. (A2,A3,A4) show reconstructed XCAT using EPTV, PCTV and hybrid-PCTV methods. (A1) is the deformed prior CT and (A5) is the ground truth. (B) are the zoomed in images of the two tumors region. From left to right columns: the deformed prior CT, EPTV, PCTV, hybrid-PCTV and ground truth. Red arrows point that hybrid-PCTV is superior to PCTV in tumor edge sharpness and orange arrows point that hybrid- PCTV is superior to EPTV in bone edge enhancement. In the third row, edge map were compared as shown in: (C1) edge weight map of the deformed prior image, (C2) weight map of last reconstruction iteration in EPTV, (C3) weight map used in PCTV, (C4) weight map used in hybrid-PCTV and (C5) weight map extracted by edge detection on the ground truth images. (D) shows the profiles along the center of the new tumor in the on-board CBCT. Red arrows point out hybrid-PCTV is superior to PCTV to enhance bone and tumor edge sharpness while orange arrows show that hybrid-PCTV is superior to EPTV to enhance bone edge sharpness. CBCT, cone-beam computed tomography; PCTV, prior contour based TV; EPTV, edge preserving TV; XCAT, extended cardiac-torso.

Table 1 Relative error and edge cross correlation of reconstructed EPTV, PCTV and hybrid-PCTV images using 30 half-fan projections

	EPTV	PCTV	Hybrid-PCTV
Relative error	1.3%	1.1%	0.9%
Edge cross correlation coefficient	0.66	0.68	0.71

PCTV, prior contour based TV; EPTV, edge preserving TV.

Figure 3C shows the edge map of these three methods compared with the ground truth edge map. As pointed by the red arrows, weight map used in hybrid-PCTV is much closer to the ground truth than the EPTV and PCTV weight map. In the EPTV method, weight map was limited by the intermediate results, which missed edge information in the spine region as indicated by the yellow arrow. PCTV weight map will have more edge information from high-quality prior CT image but may be limited by the deformable registration accuracy and mismatch between prior and on-board. As a result, the PCTV edges in the tumor regions were incorrect as indicated by the red arrows. Compared to EPTV, hybrid-PCTV inherits the advantage of PCTV with more edge information from prior images to enhance bone edge sharpness as pointed by yellow arrows. Compared with PCTV, hybrid-PCTV detected the errors in PCTV edges in the tumor regions, and corrected them using EPTV edges for accurate edge enhancement, as pointed by red arrows.

The horizontal intensity profile of the tumor and spine regions as pointed by the red and yellow arrows in *Figure 3B* were shown in *Figure 3D*. Results showed the improvement of tumor and spine edge enhancement using hybrid-PCTV method compared to the PCTV and EPTV method. *Table 1* shows the quantitative evaluation results, which demonstrated that Hybrid-PCTV method has the smallest RE and the highest edge cross correlation coefficient among all methods.

Effects of projection number

The reconstructed images of the XCAT study with different projection numbers are shown in *Figure 4A,B,C* in the axial, coronal and sagittal view. The hybrid-PCTV method provided superior results than the EPTV and PCTV methods in terms of reconstructing bones as well as small structures and enhancing tumor edge sharpness using limited projections, as indicated by orange and red arrows, respectively. To better evaluate the reconstruction performance, quantitative evaluation methods were included. The results of the whole image and local interest regions (including bone and tumors) were plotted in *Figure 4D,E,F*. Hybrid-PCTV was robust to the projection number reduction with low RE and high edge correlation. PCTV might be worse than EPTV with reducing projection number due to the inaccurate edge information of changed tumors.

Patient study using simulated CBCT projections

Figure 5A,B,C show the reconstruction results using 45 half-fan DRR of clinical patient data. Additional artificial structures indicated by red arrows were introduced in PCTV because of wrong edge information from the prior image, which was corrected in the hybrid-PCTV method. Bone sharpness was increased with PCTV and hybrid-PCTV as shown by orange arrows in *Figure 5(C2)* and *(C3)*.

Figure 5(D1,D2,D3) show the comparison of the weight map in the EPTV, PCTV and hybrid-PCTV methods, which demonstrates that hybrid-PCTV has more accurate edges than the PCTV method as indicated by the red arrows. Balance map α in *Figure 5(D4)* showed that lower weightings were assigned to PCTV in the regions with registration errors to generate a correct weight map for hybrid-PCTV.

Patient study using real CBCT projections

Figure 6 shows that deformable registration errors exist when generating on-board PCTV contours for the lung cancer patient as pointed to by the arrows. Thus, the deformed prior contour will be inaccurate in the regions with registration errors, and will lead to inaccurate edge enhancement in the PCTV method.

Figure 7A and *B* show the reconstruction results of the real lung patient projections. The half-fan projection number was reduced from 894 to 149 for the low dose reconstruction.

Tumor edge was blurred in PCTV because of deformable registration errors but was enhanced in the hybrid-PCTV with corrected edge information as red arrows pointed out

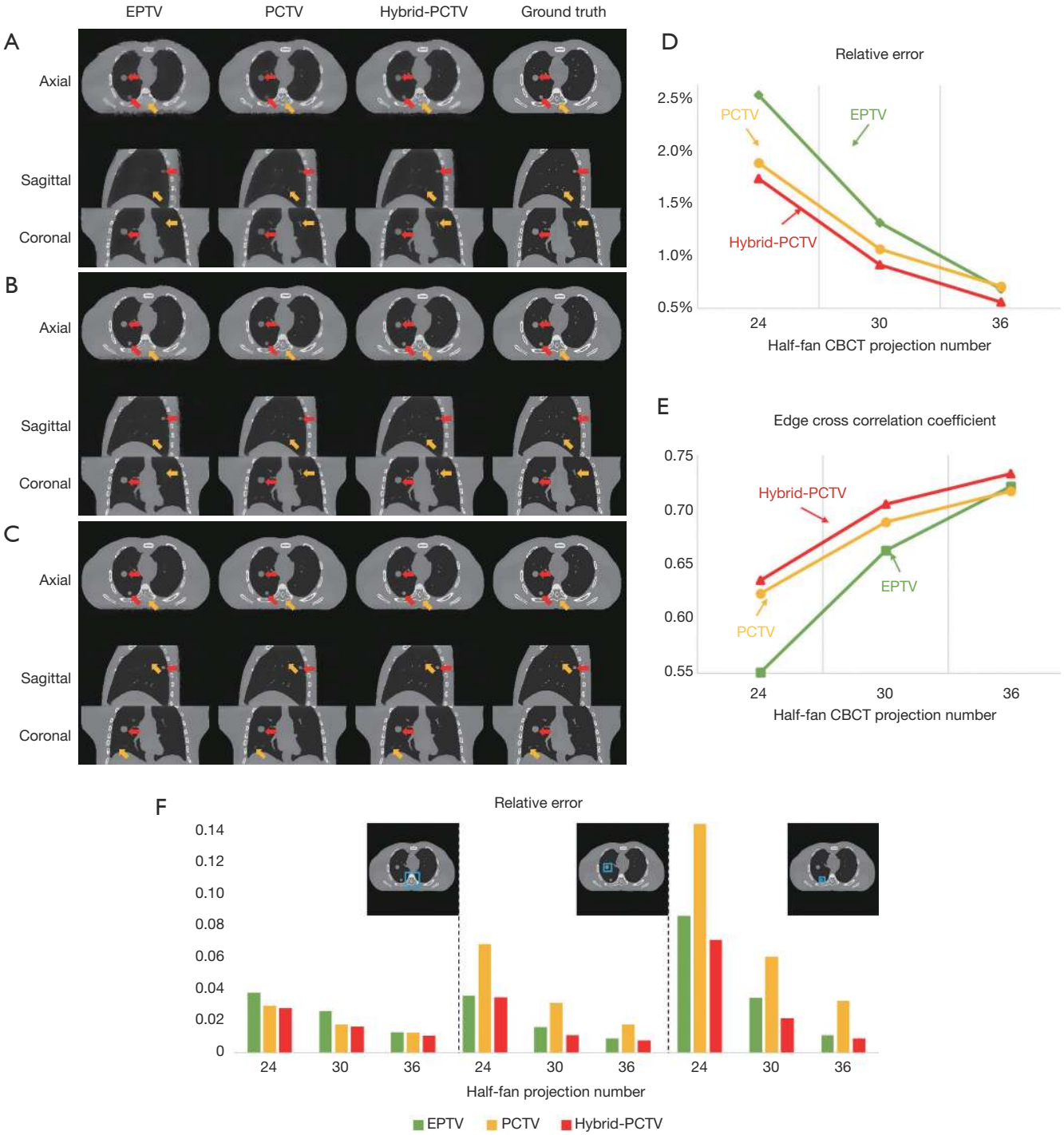

Figure 4 Comparisons of XCAT CBCT reconstructed via EPTV, PCTV and hybrid-PCTV using (A) 24 projections, (B) 30 projections and C) 36 projections. Ground truths are listed at the right column as the reference. In the quantitative evaluation, RE and edge cross correlation for EPTV, PCTV and hybrid-PCTV as functions of the number of CBCT projection number were plotted in (D) and (E), respectively. The RE of bone and tumors as blue block pointed was also calculated and was plotted in (F). CBCT, cone-beam computed tomography; PCTV, prior contour based TV; EPTV, edge preserving TV.

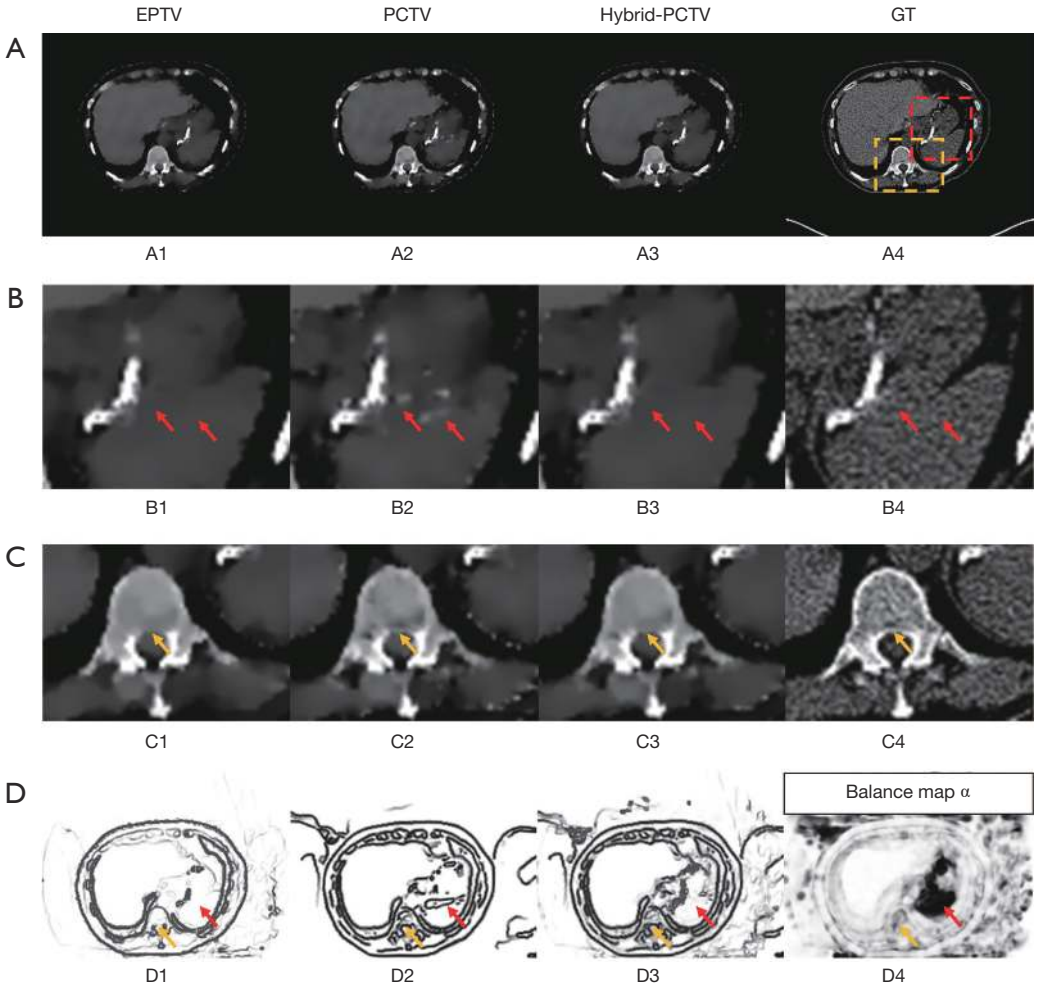

Figure 5 Reconstructed images of the liver using simulated CBCT projections. (A) Reconstructed images of the patient liver. From left to right: EPTV, PCTV, hybrid-PCTV and clinical CT as a reference. (B) Zoom in reconstruction images of red dot block in the reference while (C) zoom in reconstruction images of orange dot block in the reference. Edge map comparisons: (D1) is the weight map of last reconstruction iteration in EPTV, (D2) is the weight map used in PCTV and (D3) is the weight map used in hybrid-PCTV. (D4) is the balance map α used in the hybrid-PCTV. Red arrows point out the differences between weight map in EPTV and PCTV. PCTV, prior contour based TV; EPTV, edge preserving TV.

in *Figure 7B*. Compared to EPTV, hybrid-PCTV enhanced bone sharpness as yellow arrows pointed out in *Figure 7C*. Moreover, *Figure 7D* shows the comparison of the weight map in these methods, which demonstrates hybrid-PCTV is superior to PCTV by correcting on-board edge information based on balance map α during the reconstruction.

Figure 8 shows results for reconstruction using different projection numbers. Hybrid-PCTV can enhance the tumor and bone edge sharpness with correct edge information extracted from both PCTV and EPTV methods in all under-sampling scenarios.

Discussion

The hybrid-PCTV method combines contour information from EPTV and prior contour information from PCTV based on the similarity between on-board and deformed prior images. It corrects deformed prior contour information in the mismatched regions using the EPTV edges to account for deformable registration errors and anatomical changes between prior and on-board.

The similarity balance map α is calculated based on the SSIM method to evaluate local image similarity between on-

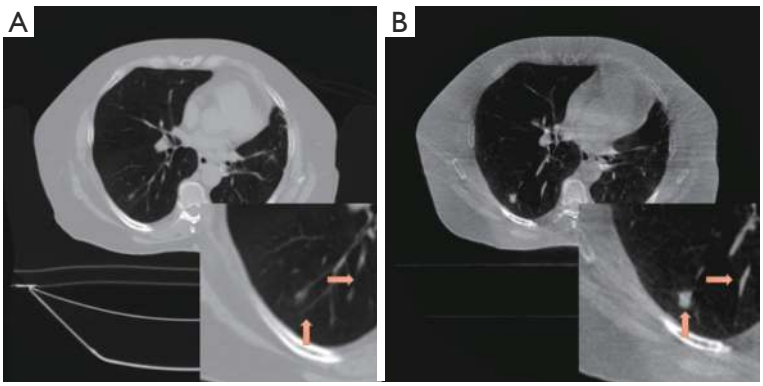

Figure 6 An example of the mismatch when deforming the prior CT image. (A) is the deformed prior CT image and (B) is the on-board full sampling CBCT images. Tumor region is zoomed in as shown in the right down corner in each image to show the mismatch because of deformable registration errors as pointed out by arrows. CBCT, cone-beam computed tomography.

board images and deformed prior images reconstructed by the same method (using EPTV in this study). The regions with the low similarity between deformed prior and on-board images might be caused by one of these two reasons: (I) deformable registration errors and (II) anatomy changes between prior and on-board (such as tumor shrinkage, new tumor, contrast agents and so on). The edge information can be corrected in the low similarity regions using edges detected by EPTV method. However, when the projection number decreases to an extremely low level, the EPTV edges in the low similarity region might also be blurred and therefore insufficient to enhance the edges in the hybrid-PCTV reconstruction.

Moreover, on-board and reference CBCT reconstructed via EPTV were used to calculate similarity balance map. Some streak artifacts in the EPTV might affect the accuracy of local similarity calculation and the propagate errors to the on-board edge weight map when extremely low projection number was used, as shown in the *Figure 3*(*C4*). Since the same reconstruction methods were used to match the image quality of on-board and deformed prior images. Thus, the impact of artifacts on SSIM calculation can be reduced. Moreover, this type of artifacts was only observed in the XCAT study where the projection number was extremely low. In the clinical study using over 45 simulated projections or over 111 real projections, no such artifacts were observed in the EPTV reconstruction. Thus, in real clinical scenarios using reasonable amount of under-sampled projections, this might be less of a problem.

The hybrid-PCTV reconstruction removes the streak artifacts typically seen in the under-sampled reconstruction by the FDK method while maintaining the edge information, which is critical for target localization in radiation therapy. However, the image contrast, especially for the soft tissue, might be still poor due to the severe scatter in CBCT. In addition, the similarity evaluation accuracy using SSIM method might be affected by the potential scattering artifacts and inadequate attenuation calibration of on-board CBCT, which might limit the accuracy of hybrid weight map generation. The image quality can be further improved by incorporating scatter correction methods (36,37) into the reconstruction framework including balance map generation.

In addition to the application in the breath-hold CBCT reconstruction, hybrid-PCTV can also be used in the 4D CBCT reconstruction which suffers streak artifacts due to under-sampled acquisition (about 200 projections in each phase). As shown in *Figure 7*, hybrid-PCTV reconstructed image in the under-sampled situation is superior to PCTV with corrected TV weight map to account for deformable registration errors. Both hybrid-PCTV and PCTV can better enhance bone edge sharpness and recover small structures in the lung region when compared to EPTV method. In the on-board 4D CBCT reconstruction, PCTV weight map for each breathing phase can be calculated from deformed 4D prior CT using phase to phase deformable registration. Then, hybrid-PCTV reconstruction will be applied to reconstruct on-board CBCT image for each phase.

Compared with previous PCTV reconstruction algorithm, the additional computational time of hybrid-PCTV is one additional EPTV reconstruction time for reference CBCT and the balance map α calculation using

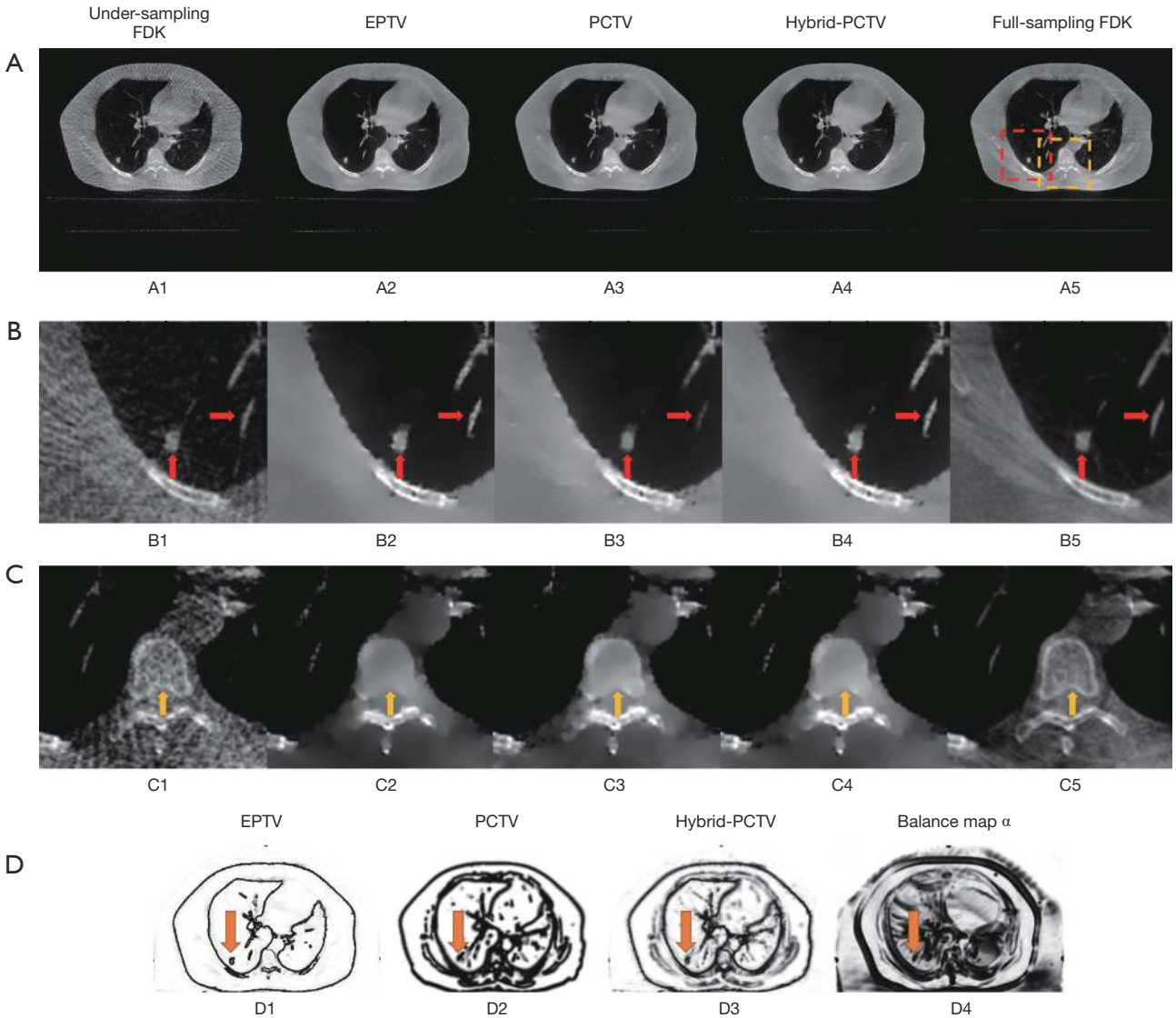

Figure 7 Reconstructed images of the lung using real CBCT projections. (A) Reconstructed images of the lung. From left to right: FDK (149 proj.), EPTV, PCTV, hybrid-PCTV and full sampling FDK (894 proj.) displayed in the window of (–800 HU, 600 HU). (B) Zoom in reconstruction images of clinical lung patient around the tumor region displayed in the window of (–800 HU, 200 HU) while (C) zoom in reconstruction images in the spine region displayed in the window of (–200 HU, 600 HU). Edge map comparisons: (D1) is the weight map of last reconstruction iteration in EPTV while (D2) is the weight map used in PCTV and (D3) is the weight map of last reconstruction iteration in hybrid-PCTV. (D4) is the balance map α based on SSIM to balance EPTV and PCTV edge during reconstruction. PCTV, prior contour based TV; EPTV, edge preserving TV.

SSIM method. The α map calculation is fast compared with the TV based reconstruction. The total reconstruction time of hybrid-PCTV can be accelerated to 1–2 minutes using parallel computing and GPU based on the previous studies (8,38-40), which makes it applicable for image-guided radiation therapy.

Conclusions

Our proposed hybrid-PCTV further improved the accuracy of edge enhancements in PCTV by accounting for uncertainties in deformable registration and anatomical mismatches between prior and on-board images. Hybrid-PCTV can be a valuable tool for low dose 3D/4D CBCT

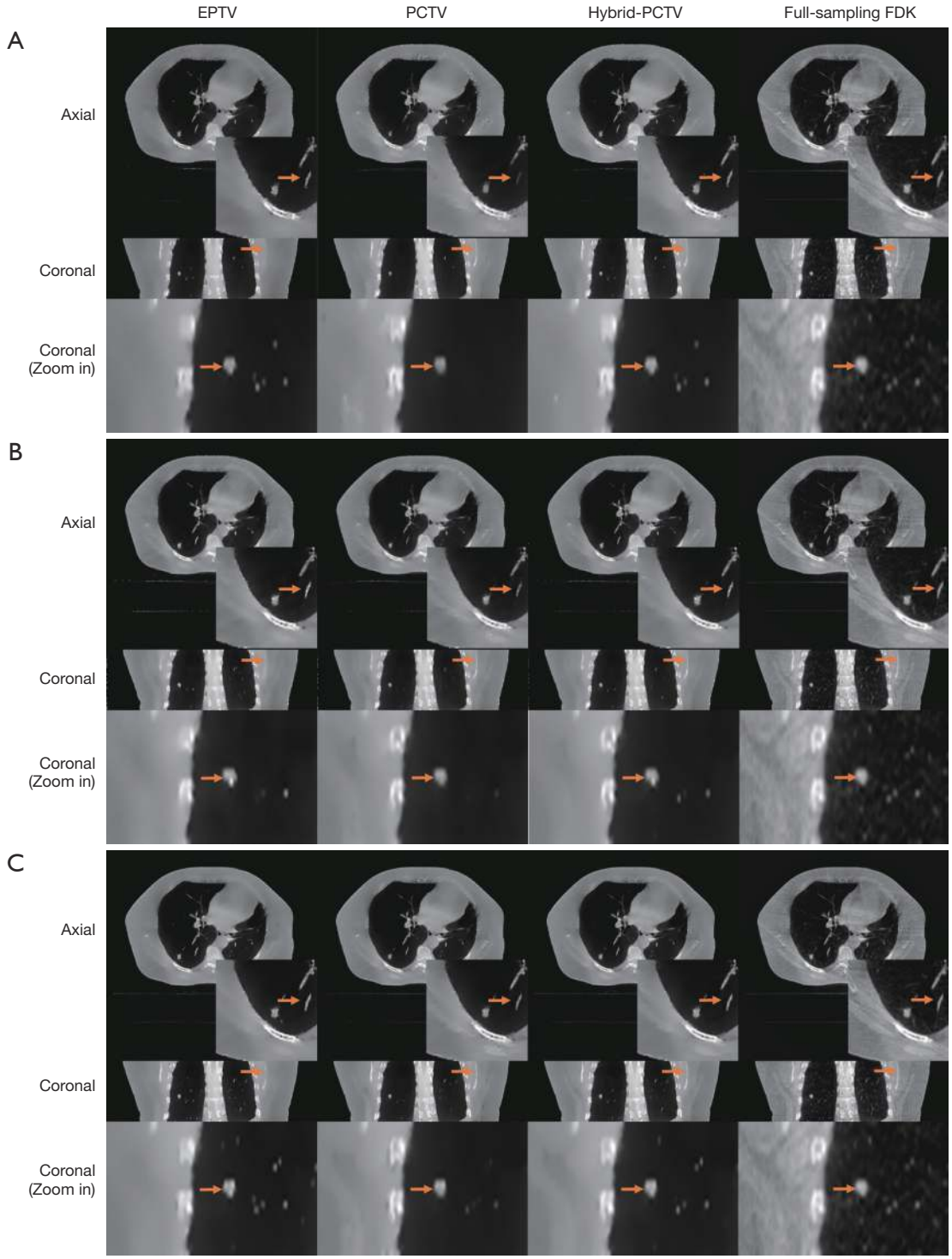

Figure 8 Comparisons of lung CBCT reconstructed via EPTV, PCTV and hybrid-PCTV using (A) 111 projections, (B) 149 projection and (C) 223 projections. Full sampling FDK using 894 half-fan projections are listed at the right column as the reference. The arrows indicate that hybrid-PCTV can enhance the edge sharpness of the tumor, small structures in the lung and bone. CBCT, cone-beam computed tomography; PCTV, prior contour based TV; EPTV, edge preserving TV.

reconstruction to improve its quality for on-board target localization in radiation therapy.

Acknowledgments

The authors would like to thank Dr. Paul Segars at Duke University for use of his XCAT digital phantom, Professor Xiaobai Sun, Professor Nikos Pitsianis, and Alexandros Iliopoulos from Duke Computer Science Department for their useful discussions about the acceleration of the system. *Funding*: This work was supported by the National Institutes of Health under Grant No. R01-CA184173.

Footnote

Conflicts of Interest: Part of the study has been presented at the American Association of Physicists in Medicine (AAPM) 60th Annual Meeting in 2018.

References

1. Cerviño LI, Chao AK, Sandhu A, Jiang SB. The diaphragm as an anatomic surrogate for lung tumor motion. Phys Med Biol 2009;54:3529-41.
2. Keall PJ, Mageras GS, Balter JM, Emery RS, Forster KM, Jiang SB, Kapatoes JM, Low DA, Murphy MJ, Murray BR. The management of respiratory motion in radiation oncology report of AAPM Task Group 76. Med Phys 2006;33:3874-900.
3. Zelefsky MJ, Kollmeier M, Cox B, Fidaleo A, Sperling D, Pei X, Carver B, Coleman J, Lovelock M, Hunt M. Improved clinical outcomes with high-dose image guided radiotherapy compared with non-IGRT for the treatment of clinically localized prostate cancer. Int J Radiat Oncol Biol Phys 2012;84:125-9.
4. Soike M, Kilburn J, Lucas J, Ayala-Peacock D, Blackstock A, Kearns W, Hinson W, Miller A, Petty W, Urbanic J. Image guided radiation therapy results in improved local control in lung cancer patients treated with fractionated radiation therapy for stage IIB-IIIB disease. Int J Radiat Oncol Biol Phys 2013;87:S547-S8.
5. Cheng HC, Wu VW, Liu ES, Kwong DL. Evaluation of radiation dose and image quality for the Varian cone beam computed tomography system. Int J Radiat Oncol Biol Phys 2011;80:291-300.
6. Santoso AP, Song KH, Qin Y, Gardner SJ, Liu C, Chetty IJ, Movsas B, Ajlouni M, Wen N. Evaluation of gantry speed on image quality and imaging dose for 4D cone-beam CT acquisition. Radiat Oncol 2016;11:98.
7. Feldkamp L, Davis L, Kress J. Practical cone-beam algorithm. JOSA A 1984;1:612-9.
8. Jia X, Lou Y, Li R, Song WY, Jiang SB. GPU-based fast cone beam CT reconstruction from undersampled and noisy projection data via total variation. Med Phys 2010;37:1757-60.
9. Sidky EY, Pan X. Image reconstruction in circular cone-beam computed tomography by constrained, total-variation minimization. Phys Med Biol 2008;53:4777-807.
10. Sidky EY, Kao CM, Pan X. Accurate image reconstruction from few-views and limited-angle data in divergent-beam CT. J Xray Sci Technol 2006;14:119-39.
11. Song J, Liu QH, Johnson GA, Badea CT. Sparseness prior based iterative image reconstruction for retrospectively gated cardiac micro-CT. Med Phys 2007;34:4476-83.
12. Niu S, Gao Y, Bian Z, Huang J, Chen W, Yu G, Liang Z, Ma J. Sparse-view x-ray CT reconstruction via total generalized variation regularization. Phys Med Biol 2014;59:2997-3017.
13. Chen Y, Yin FF, Zhang Y, Zhang Y, Ren L. Low dose CBCT reconstruction via prior contour based total variation (PCTV) regularization: a feasibility study. Phys Med Biol 2018;63:085014.
14. Tian Z, Jia X, Yuan K, Pan T, Jiang SB. Low-dose CT reconstruction via edge-preserving total variation regularization. Phys Med Biol 2011;56:5949-67.
15. Guo W, Yin W. editors. Edgecs: Edge guided compressive sensing reconstruction. Proceedings of SPIE Visual Communication and Image Processing, 2010.
16. Liu Y, Ma J, Fan Y, Liang Z. Adaptive-weighted total variation minimization for sparse data toward low-dose x-ray computed tomography image reconstruction. Phys Med Biol 2012;57:7923-56.
17. Chang M, Li L, Chen Z, Xiao Y, Zhang L, Wang G. A few-view reweighted sparsity hunting (FRESH) method for CT image reconstruction. J Xray Sci Technol 2013;21:161-76.
18. Zhu L, Niu T, Petrongolo M. Iterative CT reconstruction via minimizing adaptively reweighted total variation. J Xray Sci Technol 2014;22:227-40.
19. Wang T, Nakamoto K, Zhang H, Liu H. Reweighted Anisotropic Total Variation Minimization for Limited-Angle CT Reconstruction. IEEE Trans Nucl Sci 2017;64:2742-60.
20. Rong J, Gao P, Liu W, Liao Q, Jiao C, Lu H, editors. Prior image based anisotropic edge guided TV minimization for few-view CT reconstruction. Nuclear Science Symposium

and Medical Imaging Conference (NSS/MIC), 2014 IEEE; 2014: IEEE.
21. Qi Z, Chen GH. Extraction of tumor motion trajectories using PICCS-4DCBCT: A validation study. Med Phys 2011;38:5530-8.
22. Chen GH, Tang J, Leng S. Prior image constrained compressed sensing (PICCS): a method to accurately reconstruct dynamic CT images from highly undersampled projection data sets. Med Phys 2008;35:660-3.
23. Lee H, Xing L, Davidi R, Li R, Qian J, Lee R. Improved compressed sensing-based cone-beam CT reconstruction using adaptive prior image constraints. Phys Med Biol 2012;57:2287-307.
24. Huang J, Zhang Y, Ma J, Zeng D, Bian Z, Niu S, Feng Q, Liang Z, Chen W. Iterative image reconstruction for sparse-view CT using normal-dose image induced total variation prior. PloS One 2013;8:e79709.
25. Ren L, Zhang Y, Yin FF. A limited-angle intrafraction verification (LIVE) system for radiation therapy. Med Phys 2014;41:020701.
26. Zhang Y, Yin FF, Segars WP, Ren L. A technique for estimating 4D-CBCT using prior knowledge and limited-angle projections. Med Phys 2013;40:121701.
27. Zhang Y, Yin FF, Pan T, Vergalasova I, Ren L. Preliminary clinical evaluation of a 4D-CBCT estimation technique using prior information and limited-angle projections. Radiother Oncol 2015;115:22-9.
28. Zhang Y, Yin FF, Ren L. Dosimetric verification of lung cancer treatment using the CBCTs estimated from limited-angle on-board projections. Med Phys 2015;42:4783-95.
29. Zhang Y, Yin FF, Zhang Y, Ren L. Reducing scan angle using adaptive prior knowledge for a limited-angle intrafraction verification (LIVE) system for conformal arc radiotherapy. Phys Med Biol 2017;62:3859-82.
30. Zhang H, Gang GJ, Dang H, Stayman JW. Regularization Analysis and Design for Prior-Image-Based X-ray CT Reconstruction. IEEE Trans Med Imaging 2018;37:2675-86.
31. Nett B, Tang J, Aagaard-Kienitz B, Rowley H, Chen GH. editors. Low radiation dose C-arm cone-beam CT based on prior image constrained compressed sensing (PICCS): including compensation for image volume mismatch between multiple data acquisitions. Medical Imaging 2009: Physics of Medical Imaging; 2009: International Society for Optics and Photonics.
32. Stayman JW, Dang H, Ding Y, Siewerdsen JH. PIRPLE: a penalized-likelihood framework for incorporation of prior images in CT reconstruction. Phys Med Biol 2013;58:7563-82.
33. Dang H, Wang A, Sussman MS, Siewerdsen J, Stayman J. dPIRPLE: a joint estimation framework for deformable registration and penalized-likelihood CT image reconstruction using prior images. Phys Med Biol 2014;59:4799-826.
34. Wang Z, Bovik AC, Sheikh HR, Simoncelli EP. Image quality assessment: from error visibility to structural similarity. IEEE Trans Image Process 2004;13:600-12.
35. Segars WP, Sturgeon G, Mendonca S, Grimes J, Tsui BM. 4D XCAT phantom for multimodality imaging research. Med Phys 2010;37:4902-15.
36. Ren L, Chen Y, Zhang Y, Giles W, Jin J, Yin FF. Scatter reduction and correction for dual-source cone-beam CT using prepatient grids. Technol Cancer Res Treat 2016;15:416-27.
37. Jin JY, Ren L, Liu Q, Kim J, Wen N, Guan H, Movsas B, Chetty IJ. Combining scatter reduction and correction to improve image quality in cone-beam computed tomography (CBCT). Med Phys 2010;37:5634-44.
38. Yan H, Wang X, Shi F, Bai T, Folkerts M, Cervino L, Jiang SB, Jia X. Towards the clinical implementation of iterative low-dose cone-beam CT reconstruction in image-guided radiation therapy: Cone/ring artifact correction and multiple GPU implementation. Med Phys 2014;41:111912.
39. Pratx G, Xing L. GPU computing in Med Phys: A review. Med Phys 2011;38:2685-97.
40. Park JC, Song B, Kim JS, Park SH, Kim HK, Liu Z, Suh TS, Song WY. Fast compressed sensing-based CBCT reconstruction using Barzilai-Borwein formulation for application to on-line IGRT. Med Phys 2012;39:1207-17.

Cite this article as: Chen Y, Yin FF, Zhang Y, Zhang Y, Ren L. Low dose cone-beam computed tomography reconstruction via hybrid prior contour based total variation regularization (hybrid-PCTV). Quant Imaging Med Surg 2019;9(7):1214-1228. doi: 10.21037/qims.2019.06.02

